Heliyon 10 (2024) e40340

Contents lists available at ScienceDirect

Heliyon

journal homepage: www.cell.com/heliyon

Research article

Enzyme-free biosensor utilizing chitosan-capped ZnS doped by Mn nanomaterials for tetracycline hydrochloride detection

Son Hai Nguyen [a], Mai Thi Tran [b,c,*]

[a] School of Mechanical Engineering, Hanoi University of Science and Technology, Hanoi, 100000, Viet Nam
[b] College of Engineering and Computer Science, VinUniversity, Hanoi, 100000, Viet Nam
[c] VinUni-Illinois Smart Health Center, VinUniversity, Hanoi, 100000, Viet Nam

ARTICLE INFO

Keywords:
Zinc sulphide
Chitosan
Tetracycline
Antibiotics
Biosensors
Absorbance

ABSTRACT

Tetracycline hydrochloride is a widely used antibiotic for treating bacterial infections, but its misuse poses serious health risks. Therefore, it is crucial to accurately detect tetracycline in complex matrices. In this study, we propose a simple, enzyme-free absorbance biosensor for tetracycline detection based on the optical properties of chitosan-capped ZnS doped with Mn nanomaterials. The biosensor can detect tetracycline in a range from 13.1 pM to 72.2 pM, with the best detection limit being 2.13 pM in deionized water. It can also differentiate tetracycline from ampicillin, penicillin, cephalexin, amoxicillin, and glucose within the aforementioned range. Moreover, this novel sensor has proven reliable over time, and its performance has been demonstrated in tap water and milk. The results have the potential to revolutionize antibiotic monitoring in clinical and environmental settings, thus contributing to the global fight against antibiotic resistance.

1. Introduction

Tetracycline is a widely used antibiotic in medicine for humans, animals, and agriculture due to its broad-spectrum activity [1]. However, its pervasive use has led to widespread environmental dissemination and increased antibiotic-resistant bacteria, pressing global health concerns [2]. Hence, detecting tetracycline residues in various ecosystems is crucial for monitoring and managing its environmental impact, ensuring food safety, and maintaining the efficacy of antibiotics. Current antibiotic detection methods, including microbiological assays, mass spectrometry, and High-Performance Liquid Chromatography (HPLC), have significant limitations [3–5]. While microbiological assays are simpler and more cost-effective, they lack the precision and specificity required to discriminate between antibiotics or accurately measure concentrations. Mass spectrometry has excellent precision, but its high cost and complex methodology limit its use for widespread and rapid testing. HPLC, though sensitive, is costly, labor-intensive, time-consuming, and requires expert operators for reliable results. Furthermore, these approaches frequently necessitate sample pretreatment, which adds to the detection time. Thus, developing sensitive, accurate, and accessible detection methods for tetracycline is a significant step toward safeguarding public health and preserving the effectiveness of this essential class of antibiotics.

Researchers are developing nanomaterial-based biosensors to overcome the limitations of traditional antibiotic detection methods [6]. These biosensors have gained popularity due to their specificity, sensitivity, and speed [7–10]. Using the excellent optical characteristics of nanomaterials, optical biosensors have emerged as a promising tool for antibiotic monitoring. Over the past decades,

* Corresponding author. College of Engineering and Computer Science, VinUniversity, Hanoi, 100000, Viet Nam.
E-mail address: mai.tt@vinuni.edu.vn (M.T. Tran).

https://doi.org/10.1016/j.heliyon.2024.e40340
Received 31 July 2024; Received in revised form 11 November 2024; Accepted 11 November 2024

many studies have explored the use of nanomaterials in optical biosensors for antibiotic detection. For instance, fluorescent biosensors have used graphene oxide and aptamer to detect oxytetracycline, and CdTe quantum dots combined with antibodies to detect tetracycline and penicillin G [11–13]. Colorimetric biosensors have also been applied to detect oxytetracycline, tetracycline, and doxycycline, utilizing Fe_3O_4 magnetic nanoparticles with enzyme [14] or carbon dots [15–17], or rare earth multicolor fluorescent probe Eu [18–20]. Another example is biosensors based on gold nanoparticles, antibodies, and surface plasmon resonance measurements. They have been widely used to detect fluoroquinolone and chloramphenicol [21]. While optical nanomaterial-based biosensors offer numerous advantages for antibiotic detection, their development is still ongoing, with significant potential for advancements in sensor design. Incorporating diverse nanomaterials could enhance these sensors' sensitivity, selectivity, detection range, and limit of detection (LOD) while reducing costs and simplifying the preparation process.

Zinc sulfide-doped manganese (ZnS:Mn) exhibits strong photoluminescence, making it effective for detecting target analytes such as antibiotics [22,23]. Chitosan, a naturally occurring polysaccharide, is biocompatible, non-toxic, and contains various functional groups that can immobilize bioreceptors [24]. Taking advantage of both ZnS:Mn and chitosan, chitosan-capped ZnS doped with Mn ((Mn:ZnS)CS) nanoparticles with unique physicochemical features and biocompatibility have been used as antibiotic biosensors [25,26]. However, in these works, enzymes were required to enhance the specificity. Enzyme-based sensors for detecting antibiotics have several drawbacks, including sensitivity to environmental conditions like temperature and pH, which can affect their accuracy. They can also be costly due to the need for pure, stable enzymes and often have a limited shelf life. Moreover, these sensors might require specific conditions or multiple enzyme types to detect various antibiotics, and their susceptibility to inhibition can lead to false negatives. Generally, enzyme-based sensors are not reusable, increasing costs and generating waste.

Despite these promising results, no studies have employed chitosan-capped ZnS-doped Mn nanoparticles to detect tetracycline. Moreover, no previous research has focused explicitly on absorbance biosensors for tetracycline detection. Absorbance biosensors are crucial in bioanalytics, medical diagnostics, and environmental monitoring due to their high sensitivity, real-time monitoring capabilities, and cost-effectiveness. They operate by measuring changes in light absorbance resulting from specific biomolecular interactions, enabling the detection of small concentrations of target substances such as glucose, toxins, and pathogens, as highlighted by prior studies [27,28]. Our research addresses this gap by developing a novel, enzyme-free absorbance biosensor using chitosan-capped ZnS nanoparticles for tetracycline detection. This study is the first to report on a tetracycline absorbance biosensor based on these nanoparticles, with a detection range of 13.1–72.2 pM and a detection limit of 2.13 pM. We also evaluate the performance of the proposed sensors in detecting tetracycline in complex matrices, such as tap water and milk. Additionally, the high selectivity of the biosensors, particularly against common antibiotics like ampicillin, penicillin, amoxicillin, cephalexin, and non-antibiotic compounds like glucose, is further explored. One key advantage of this system is its ability to perform label-free detection, reducing both preparation time and potential interference. The simplicity of the biosensor design, which typically involves only a light source, sample holder, and detector, makes it a cost-effective and accessible solution for healthcare and environmental safety applications. Furthermore, technological advancements have enabled the development of miniaturized, portable versions, allowing for point-of-care testing and field monitoring, thereby expanding its accessibility and practical utility.

2. Materials and methods

2.1. Chemicals

The chemicals used to prepare the sensing materials were reported in our previous works [29,30]. They include chitosan, manganese chloride tetrahydrate, zinc acetate dihydrate, and ethanol. The analytes are tetracycline hydrochloride (ultra-pure, $C_{22}H_{24}N_2O_8$.HCl, Biobasic, Canada), D-glucose monohydrate (99.99 %, $C_6H_{12}O_6.H_2O$, Biobasic, Canada), penicillin G sodium salt (ultra-pure, $C_{16}H_{17}N_2NaO_4S$, Bomeibio, China), ampicillin sodium salt (99.99 %, $C_{16}H_{18}N_3NaO_4S$, Njduly, China), cephalexin monohydrate (98 %, $C_{16}H_{19}N_3O_5S{\cdot}H_2O$, Macklin, Shanghai, China), amoxicillin crystalline (99 %, $C_{16}H_{19}N_3O_5S$, Macklin, Shanghai, China).

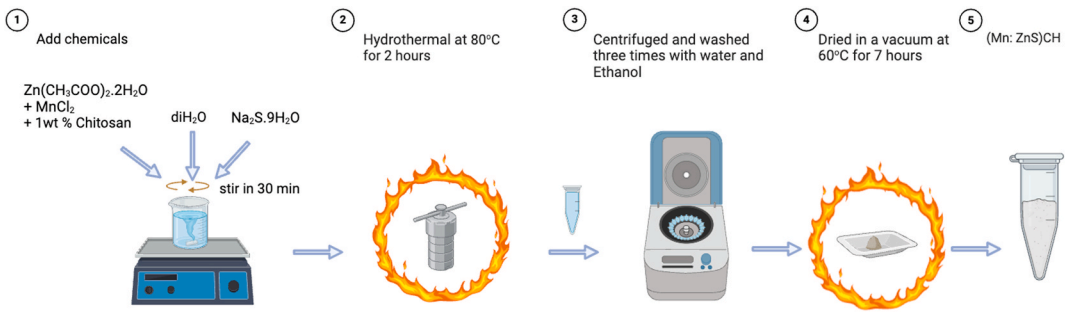

Fig. 1. Schematic of the preparation of (Mn:ZnS)CS materials by the hydrothermal method.

2.2. Nanomaterial preparation

We used the hydrothermal method to synthesize Chitosan-capped ZnS doped Mn ((Mn:ZnS)CS), adhering to the protocol outlined in previous works [29,30], as shown in Fig. 1. First, we prepared a solution of 1.5 % chitosan in 1 % acetic acid. We then mixed zinc acetate with manganese chloride in a 10:1 M ratio and stirred until fully dissolved. Next, we incrementally introduced a chitosan and sodium sulfide suspension into the mixture, stirring continuously for half an hour. Then, this mixture was placed in a Teflon autoclave and heated to 80 °C for 2 h. The resulting precipitate was washed with ethanol and centrifuged five times. Finally, the product was dried for 7 h at 60 °C to complete the process.

2.3. Absorbance measurements

In our experiment, we added a volume of sensing materials, specifically 500 mg/L (Mn:ZnS)CS, into cuvettes. We then incrementally added the analytes to the cuvette to achieve the desired concentrations, ranging from 13.1 to 72.2 pM. The absorbance at

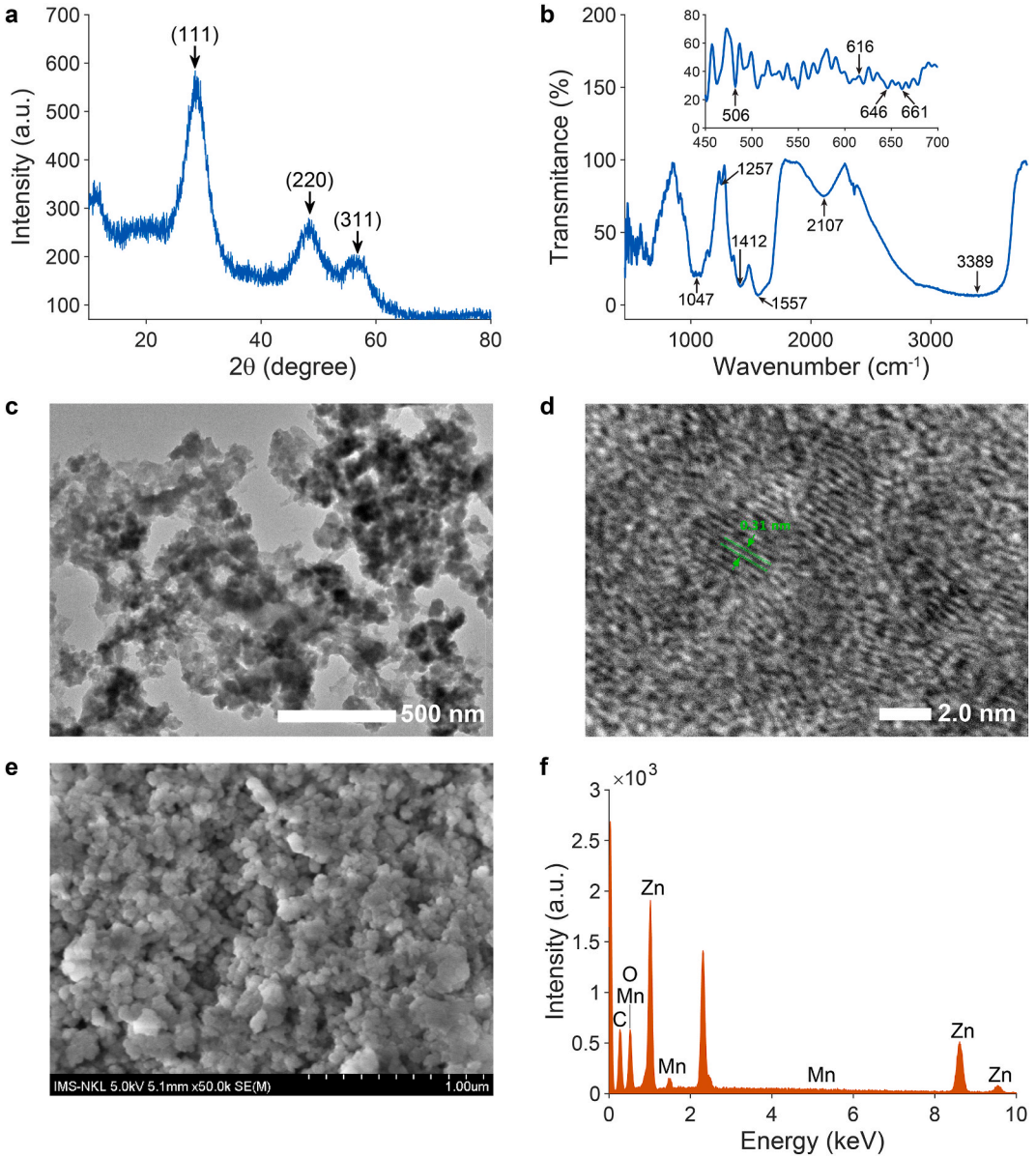

Fig. 2. Characterizations of structure and morphology of prepared (Mn:ZnS)CS. (**a**) XRD pattern taken by Rigaku MiniFlex600 (Rigaku Europe SE, Germany). (**b**) FTIR spectrum acquired by FTIR Jasco 4600 spectrometer (Jasco, Japan). (**c**, **d**) TEM images captured by JEM 2100 (JEOL Ltd., Japan). (**e**, **f**) SEM and EDX images taken using HITACHI S-4800 (Hitachi High-Tech, Japan).

each concentration was measured using a DeNovix UV–Vis spectrometer.

3. Results and discussion

3.1. Characterizations of synthesized material

The structure of prepared materials was characterized using the XRD and FTIR analysis. Fig. 2a illustrates the cubic sphalerite structure of ZnS with three peaks at positions (111), (220), and (311) (JCPDS card No.5-0566). Mn^{2+} and chitosan did not induce clear peaks in the XRD pattern due to a small doping percentage. In addition, FTIR analysis of the material (Fig. 2b) confirmed the presence of Mn and chitosan. The vibrational modes of chitosan include N-H bend at 3389 cm^{-1}, -C-O at 1412 and 1557 cm^{-1}, and C-O-C bond at 1047 cm^{-1}. The peaks of ZnS were observed at 508, 616, and 1047 cm^{-1}. Mn was detected at 661 cm^{-1} and split peaks at 1047 cm^{-1}. The structure of prepared materials was also confirmed in Fig. 2d, in which the typical lattice spacing is 0.31 nm, corresponding to the ZnS and EDX image in Fig. 2f. The morphology and size of synthesized materials were shown in the TEM image (Fig. 2c), and SEM image (Fig. 2e). SEM images of the prepared material as nanoparticles and the TEM image showed that the size of nanoparticles around 50 nm. Furthermore, in the TEM image, no individual particle was detected, likely due to the chitosan-coated on the (Mn:ZnS) surface, which is a polymer that binds particles together.

3.2. Direct detection of tetracycline by absorbance measurements

In this section, the sensitivity of the proposed sensors to tetracycline (TET) in the range of 13.1 pM–72.2 pM is studied. First, absorbance measurements were performed when the biosensors were exposed to different concentrations of TET (Fig. 3a) and deionized (DI) water (Fig. 3b). The absorbance spectra of TET in DI are shown in Fig. 3c. When the sensors interacted with TET, the absorbance varied depending on the wavelength. Four isosbestic points at 260, 295, 330, and 405 nm were observed in Fig. 3a, which separate the enhancing and quenching effects. The enhancing effect between 330 and 405 nm and the peak at 365 nm was particularly utilized for further investigation. This effect is attributed to the interaction between TET and the proposed sensors, as confirmed by the absorbance measurements of the sensors in contact with DI (Fig. 3b). Clearly, no enhancement was observed without TET, and the absorbance of TET itself was negligible (Fig. 3c). Therefore, we can conclude that the proposed biosensors are capable of detecting TET within the range of 13.1–72.2 pM using a linear fitting function ($R^2 = 0.999$), as shown in Fig. 3d:

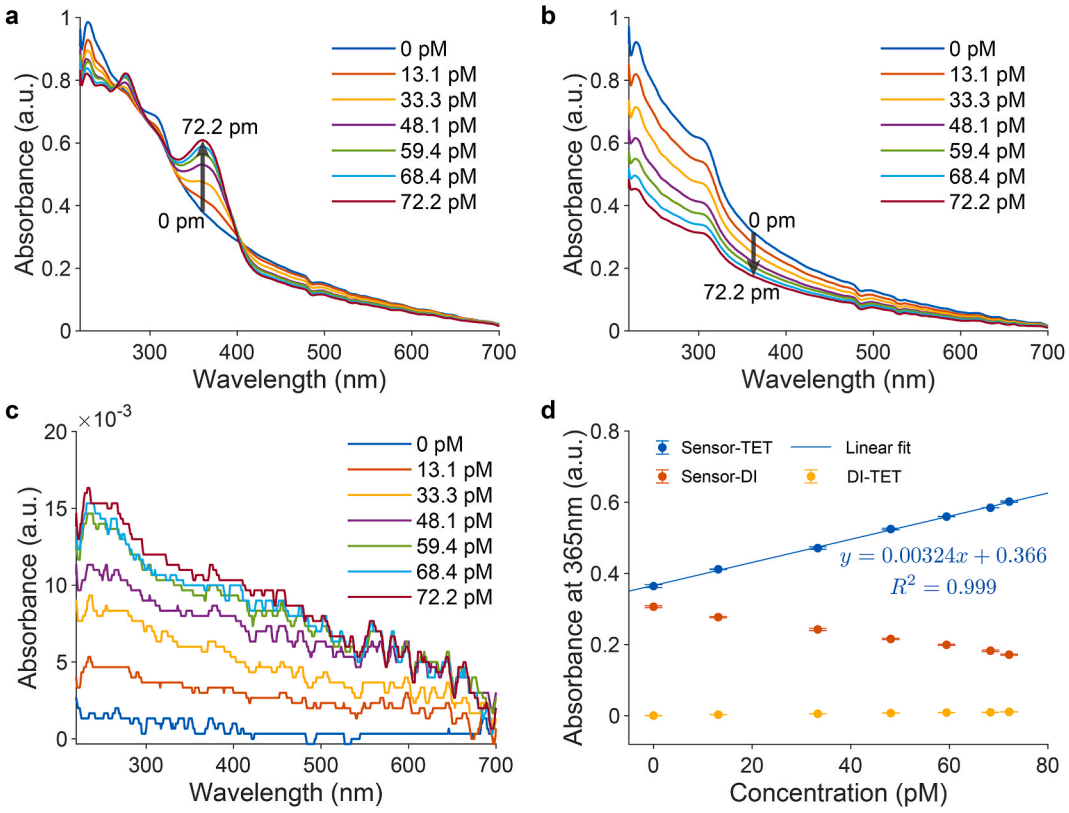

Fig. 3. Absorbance spectra of (**a**) proposed biosensors with various tetracycline concentrations, (**b**) sensors with equivalent amounts of DI water, and (**c**) different TET concentrations. (**d**) Dependency of absorbance at 365 nm wavelength on analytes' concentrations in experiments (**a**–**c**).

$$y = 0.00324x + 0.366 \quad (1)$$

where y denotes the measured absorbance at 365 nm, x is the concentration of TET (pM).

Furthermore, the proposed sensors were tested for stability over four weeks. The results are shown in Fig. 4a. Obviously, the relationship between the absorbance at 365 nm and TET concentrations remained stable and nearly unchanged over time. To aid visualization, we define the absorbance change before and after adding 72.2 pM of TET as shown in Eq. (2):

$$\Delta I = 100\% \times \frac{I - I_0}{I_0} \quad (2)$$

where I_0 is the absorbance at 365 nm before adding TET, and I is the absorbance at 365 nm after adding 72.2 pM of TET. The result shown in Fig. 4b again verified the remarkable stability of the proposed biosensors over four weeks, with the potential for a longer time.

To validate the accuracy of the proposed biosensors, we prepared several test samples with known concentrations. Then, the absorbances at 365 nm of the sensors were recorded upon adding the test samples to the sensors. These measured absorbances were then used to calculate the concentrations of the test samples using Eq. (1). The results, shown in Table 1, demonstrate that the estimated concentrations closely matched the actual concentrations of the test samples, with all differences being less than 10 %. Moreover, the accuracy of the calculated concentrations improved as the sample concentrations increased.

3.3. Selectivity of tetracycline biosensors utilizing (Mn:ZnS)CS nanomaterials

To explore the selectivity property of the proposed sensor, we exposed it to different analytes, including common antibiotics such as ampicillin (AMP), penicillin (PCN), amoxicillin (AMX), cephalexin (CEX), and a non-antibiotic, glucose. The experiments and analysis were repeated as described in Section 3.2. The absorbance spectra are shown in Supplement S1. Only TET induced both enhancing and quenching effects, while the other analytes exhibited only quenching effects. Therefore, this simple sensor can easily differentiate TET from the other tested analytes. Fig. 5 clearly shows the enhancing effect of the sensors in the presence of TET, reflected by a positive slope, whereas all other analytes showed negative slopes (Fig. 5a). The same observation was also displayed in Fig. 5b when only TET produced a positive ΔI. This result will pave the way for further work in utilizing the proposed sensor in different working environments, which will be discussed in Section 3.4.

As discussed earlier, this simple sensing platform can easily detect TET with high selectivity and stability without any enzymes. This outstanding result is due to the sensing materials. To explore this further, we prepared different sensing materials using the same protocol but omitted chitosan. The structure and morphology of this material are shown in Supplement S2. The sensors based on (Mn:ZnS) were tested with TET, and the results are displayed in Fig. 6. Fig. 6a shows the quenching effect of the sensors-based (Mn:ZnS) when exposed to TET, which differs from the behavior of the proposed sensors ((Mn:ZnS)CS-based sensors). This difference is more evident in Fig. 6b, where the operation line of (Mn:ZnS)CS-based sensors has a positive slope, while (Mn:ZnS)-based sensors exhibit a negative slope. The absorbance values for the reference sensors (Mn:ZnS-based sensors) were small (around 0.2) and changed slightly. After adding 72.2 pM and before adding TET, the difference was positive (65 %) for the proposed sensor but negative (−12 %) for the reference one (Fig. 6c).

These results demonstrate that chitosan is crucial to the functionality of the proposed sensor. The functional groups on chitosan, particularly the hydroxyl amino groups, likely play a key factor in its various characteristics. These include its reduction capabilities, which facilitate the creation of microparticles, and its potential to form bonds with tetracycline through electrostatic forces, hydrogen bonding, or covalent interactions, as illustrated in Fig. 7. The absorbance changes that encompass both quenching and enhancing effects when tetracycline hydrochloride interacts with chitosan-coated ZnS doped with Mn across different wavelengths can be

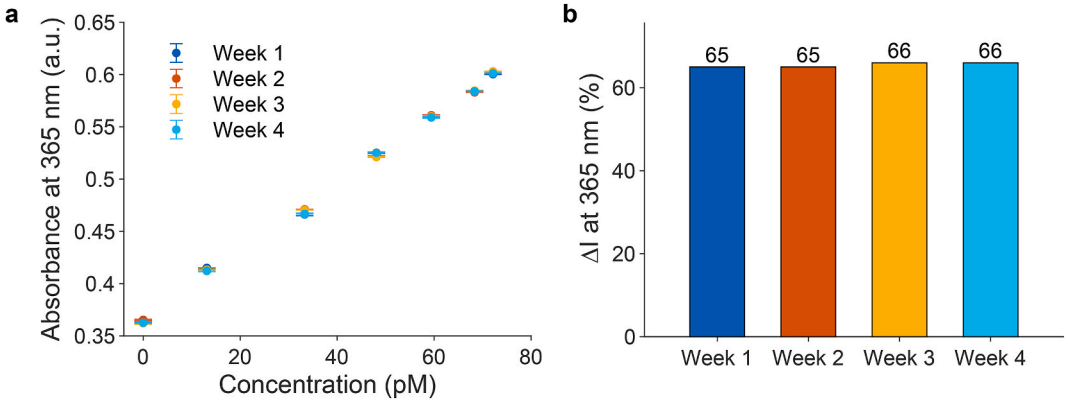

Fig. 4. Demonstration of the proposed sensors' high stability. (**a**) The measured absorbance at 365 nm with different TET concentrations over four weeks, (**b**) Histogram of absorbance changes (ΔI) at 365 nm over four weeks.

Table 1
Verification of operation function of proposed sensors.

Actual concentration (pM)	Measured absorbance at 365 nm (a.u.)	Estimated concentration (pM)	Difference (%)
24.05	0.45	25.91	7.72
41.23	0.50	43.06	4.44
54.11	0.54	55.63	2.80
64.13	0.58	65.73	2.49

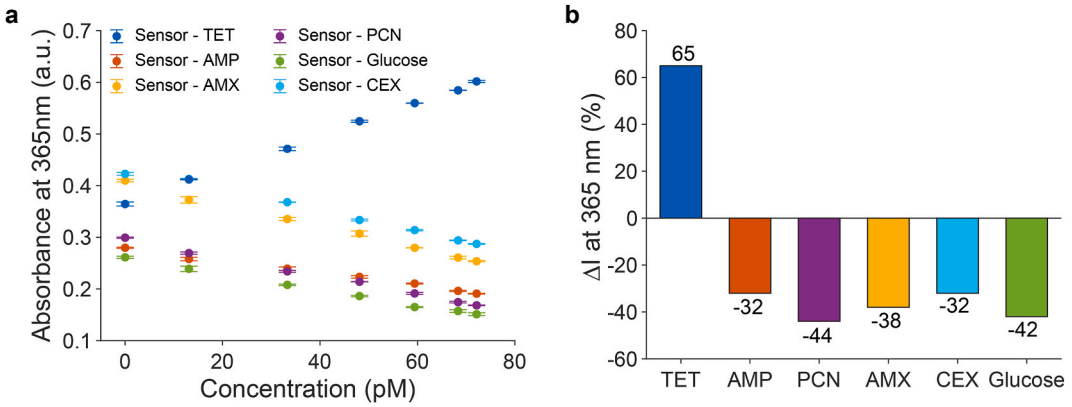

Fig. 5. Selectivity of the proposed sensors over different analytes, including AMP, AMX, PCN, CEX, and Glucose: (**a**) Absorbance at 365 nm with different analyte's concentration, (**b**) ΔI at 365 nm when different analytes are added to proposed biosensors. Only TET induced positive ΔI.

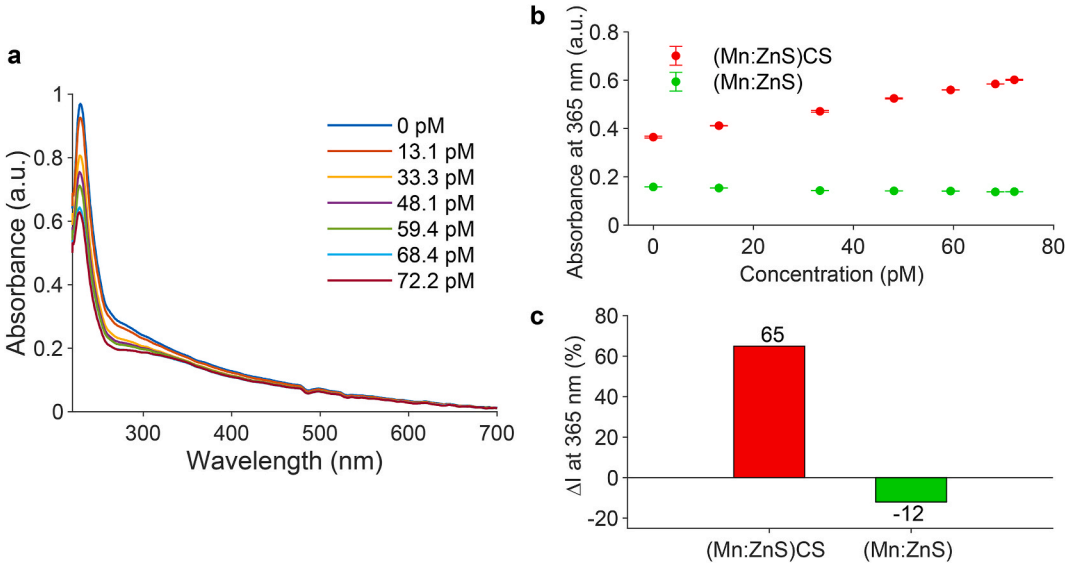

Fig. 6. Absorbance measurements of sensors based on (**a**) (Mn:ZnS) nanomaterials, (**b**) Dependence of absorbance at 365 nm on tetracycline concentrations, derived from Figs. 3a and 6a. (**c**) ΔI was at 365 nm when sensors were in contact with TET.

explained through the complex interplay of photophysical interactions at the nanoparticle-biomolecule interface. With its active hydroxyl and amino groups, the chitosan matrix provides a reactive surface for tetracycline to bind, potentially through electrostatic attraction, hydrogen bonding, or covalent linkages. This binding modulates the electronic properties of the ZnS:Mn nanoparticles by altering the local electronic states and the distribution of electronic density at the surface. At specific wavelengths, the bound tetracycline molecules may promote more efficient electronic transitions than those in the unbound state, leading to enhanced absorbance due to the formation of new sub-bandgap states or the alteration of existing ones [26,31–33].

Conversely, the tetracycline may induce a quenching effect at other wavelengths by introducing non-radiative decay pathways or perturbing the electronic structure to inhibit specific transitions. The doping of Mn within the ZnS lattice creates defect states that are sensitive to such surface modifications, resulting in a spectral shift or a change in absorbance intensity. Moreover, surface plasmon

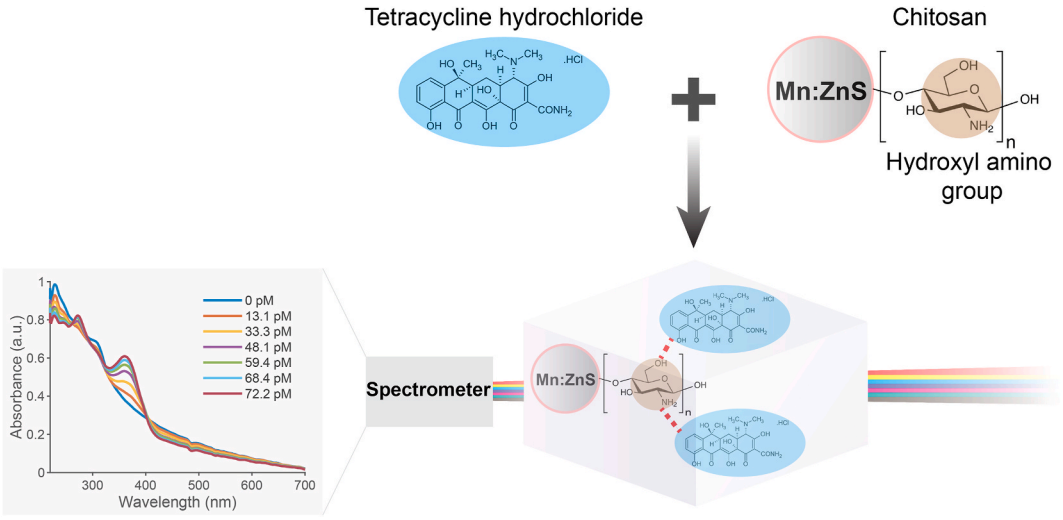

Fig. 7. Schematic of the proposed absorbance sensors' sensing mechanism.

resonance (SPR) can also contribute to the observed spectral changes. When the nanoparticles interact with tetracycline, their dielectric properties may be altered, affecting the SPR conditions and leading to wavelength-dependent variations in absorbance.

3.4. Testing the working performance of proposed biosensors in a different medium

To validate the effectiveness of proposed sensors for TET detection in complex matrices, TET was dissolved in tap water (supplied by Hanoi Water Limited Company) and diluted organic milk with concentrations from 13.1 to 72.2 pM. The absorbance spectra of sensors in contact with two samples are shown in Fig. 8a and b. The absorbances at 365 nm respective to TET concentration were measured and are presented in Fig. 8c. All experimental data can be fitted with linear functions with high precision ($R^2 \approx 1$), as shown in Table 2, with positive slopes indicating enhancing effects. However, the slopes were shallow for clean water and milk, especially for milk (0.0006). The detection limits were 2.13 pM for DI water, 6.21 pM for milk, and 11.03 pM for tap water. The absorbance changes at 365 nm for clean water and milk were reduced to 17 % and 14 %, respectively, as shown in Fig. 8d. These promising results suggest potential optimization steps for future works, including adjusting the sensing material concentrations, modifying the preparation methods to alter the structures and morphology of the sensing materials, and incorporating aptamers like enzymes and antibodies.

This study demonstrated a simple and powerful sensing platform that requires no enzymes, antibodies, DNA, or other bioreceptors. The measurement setup is not only simple but also portable. With high sensitivity, stability, and promising selectivity, this proposed sensor offers several advantages over previously reported TET biosensors. For example, Zhang et al. used a fluorescence TET chemosensor utilized the hybrid ZnS:Mn QDs with mesoporous silica and molecularly imprinted polymer in the range of 0.113–2.25 μM and LOD of 3.375×10^{-2} μM which is higher than our test ranges and LOD [34]. Using the same approach of absorbance measurement, Yang et al. used aptamer with silver clusters to detect TET from 20 μg/L to 10 kg/L with an LOD of 11.46 μg/L, which is significantly higher than our proposed system [35]. Another method using a colorimetric aptasensor, which is based on aptamers and gold nanoparticles, achieved a LOD of 266 pM. However, its quantitative measurement capabilities were limited, and the sensor was relatively expensive [36]. In a different method, an electrochemical TET aptasensor based on a graphene oxide nanosheet-modified glassy carbon electrode was reported. In this work, under optimum conditions, the EIS aptasensor can detect TET from 1.0×10^{-7} to 10 μM with a LOD of 2.9×10^{-8} μM. DPV aptasensor also can detect TET from 1.0×10^{-4} to 100 μM with a LOD of 3.1×10^{-5} μM [37]. This LOD was also higher than the proposed sensors in this report. Thus, our work offers significant improvements in sensitivity, cost-efficiency, and simplicity compared to existing TET detection methods.

This study serves as a proof of concept for a simple and efficient biosensor to detect tetracycline; however, several limitations that could affect its broader application must be acknowledged. While the biosensor demonstrates high selectivity for tetracycline, it has not been tested for detecting a wider range of antibiotics, which may limit its utility in comprehensive antibiotic surveillance. In addition, its performance in complex biological matrices, such as blood or urine, remains unexamined, which could restrict its applicability in clinical settings. To expand the sensor's utility and enhance its practical effectiveness, these limitations need to be addressed. In future work, we plan to evaluate the biosensor's performance in the presence of interferences from biological small molecules typically found in real environments and complex matrices. We also aim to test the sensor under different conditions, such as varying temperatures and pH levels, to further assess its robustness and reliability.

4. Conclusions

In conclusion, enzyme-free tetracycline biosensors were successfully developed using low-cost (Mn:ZnS)CS nanomaterials and

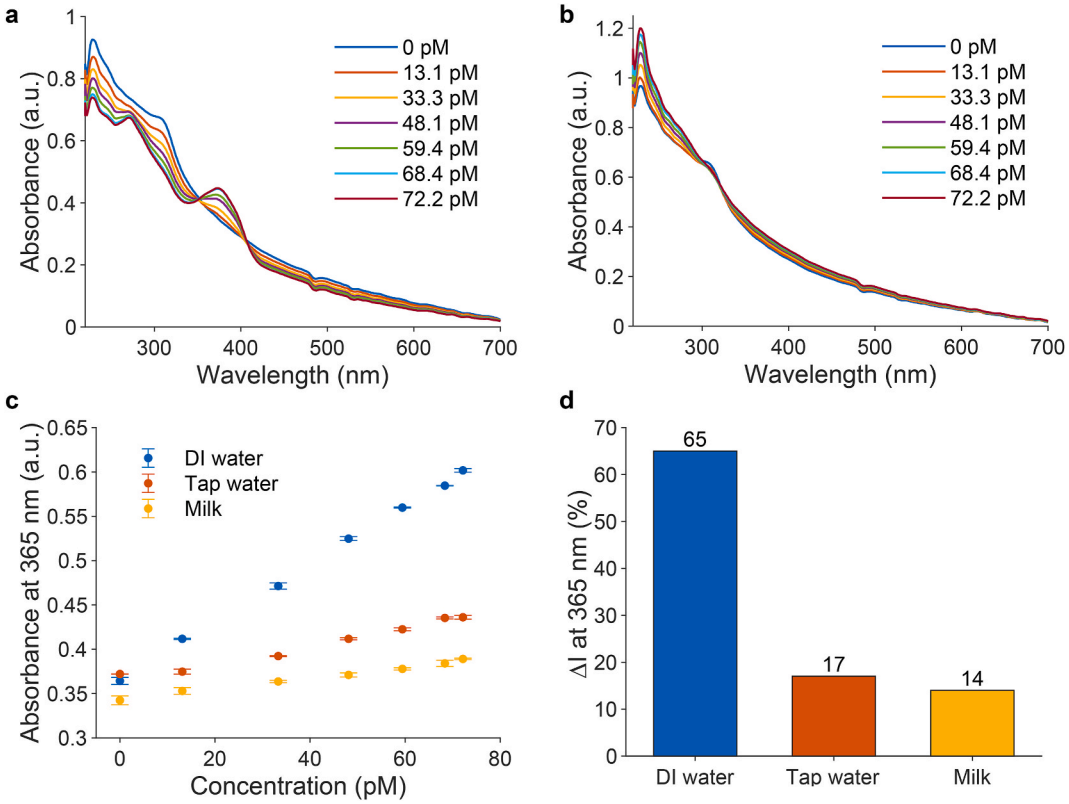

Fig. 8. Absorbance measurements of proposed biosensors in (**a**) tap water, (**b**) diluted organic milk. (**c**) Relationship between absorbance at 365 nm of the proposed sensors and tetracycline concentrations in different matrices. (**d**) ΔI at 365 nm when the sensors were in contact with tetracycline.

Table 2
Performance of the proposed sensors in different environments.

Working environment	Operating function	R^2	LOD (pM)
DI water	$y = 0.0032x + 0.3661$	0.999	2.13
Tap water	$y = 0.001x + 0.3659$	0.978	11.03
Milk	$y = 0.0006x + 0.3433$	0.993	6.21

simple absorbance measurements. The proposed biosensors demonstrated high accuracy, stability, and sensitivity in detecting tetracycline within the range of 13.1 pM–72.2 pM. These biosensors also achieved the best detection limit of 2.13 pM, which is impressive for a simple, non-enzyme absorbance biosensor. Overall, the promising results of this study will pave the way for further research into the use of (Mn:ZnS)CS for real-time antibiotic detection. This achievement could significantly facilitate antibiotic monitoring.

CRediT authorship contribution statement

Son Hai Nguyen: Writing – review & editing, Writing – original draft, Visualization, Validation, Methodology, Investigation, Formal analysis, Conceptualization. **Mai Thi Tran:** Writing – review & editing, Writing – original draft, Visualization, Validation, Supervision, Resources, Project administration, Methodology, Investigation, Funding acquisition, Formal analysis, Conceptualization.

Data availability

All data are included in the manuscript and the supplementary information.

Funding

Funding: This research is funded by the Fast Track grant of VinUniversity to MTT.

Declaration of Competing Interest

The authors declare that they have no known competing financial interests or personal relationships that could have appeared to influence the work reported in this paper.

Acknowledgments

The authors thank the former member of BEL Lab at VinUniversity, Van-Nhat Nguyen, for supporting this work.

Appendix A. Supplementary data

Supplementary data to this article can be found online at https://doi.org/10.1016/j.heliyon.2024.e40340.

References

[1] I. Chopra, M. Roberts, Tetracycline antibiotics: mode of action, applications, molecular biology, and epidemiology of bacterial resistance, Microbiol. Mol. Biol. Rev. 65 (2) (2001) 232–260, https://doi.org/10.1128/mmbr.65.2.232-260.2001.
[2] B. Berglund, Environmental dissemination of antibiotic resistance genes and correlation to anthropogenic contamination with antibiotics, Infect. Ecol. Epidemiol. 5 (1) (2015) 28564, https://doi.org/10.3402/iee.v5.28564.
[3] T. Gallagher, et al., Liquid chromatography mass spectrometry detection of antibiotic agents in sputum from persons with cystic fibrosis, Antimicrob. Agents Chemother. 65 (2) (2021), https://doi.org/10.1128/aac.00927-20, 10.1128/aac. 00927-20.
[4] I. Varenina, N. Bilandžić, Đ.B. Luburić, B.S. Kolanović, I. Varga, High resolution mass spectrometry method for the determination of 13 antibiotic groups in bovine, swine, poultry and fish meat: an effective screening and confirmation analysis approach for routine laboratories, Food Control 133 (2022) 108576, https://doi.org/10.1016/j.foodcont.2021.108576.
[5] Z.A. Khan, M.F. Siddiqui, S. Park, Current and emerging methods of antibiotic susceptibility testing, Diagnostics 9 (2) (2019) 49, https://doi.org/10.3390/diagnostics9020049.
[6] C. Zhou, H. Zou, C. Sun, Y. Li, Recent advances in biosensors for antibiotic detection: selectivity and signal amplification with nanomaterials, Food Chem. 361 (2021) 130109, https://doi.org/10.1016/j.foodchem.2021.130109.
[7] N. Lu, J. Chen, Z. Rao, B. Guo, Y. Xu, Recent advances of biosensors for detection of multiple antibiotics, Biosensors 13 (9) (2023) 850, https://doi.org/10.3390/bios13090850.
[8] A. Joshi, K.-H. Kim, Recent advances in nanomaterial-based electrochemical detection of antibiotics: challenges and future perspectives, Biosens. Bioelectron. 153 (2020) 112046, https://doi.org/10.1016/j.bios.2020.112046.
[9] G. Cacciatore, M. Petz, S. Rachid, R. Hakenbeck, A.A. Bergwerff, Development of an optical biosensor assay for detection of β-lactam antibiotics in milk using the penicillin-binding protein 2x, Anal. Chim. Acta 520 (1–2) (2004) 105–115, https://doi.org/10.1016/j.aca.2004.06.060.
[10] D. Sadighbayan, M. Hasanzadeh, E. Ghafar-Zadeh, Biosensing based on field-effect transistors (FET): recent progress and challenges, TrAC, Trends Anal. Chem. 133 (2020) 116067, https://doi.org/10.1016/j.trac.2020.116067.
[11] B. Tan, H. Zhao, L. Du, X. Gan, X. Quan, A versatile fluorescent biosensor based on target-responsive graphene oxide hydrogel for antibiotic detection, Biosens. Bioelectron. 83 (2016) 267–273, https://doi.org/10.1016/j.bios.2016.04.065.
[12] E. Song, et al., Multi-color quantum dot-based fluorescence immunoassay array for simultaneous visual detection of multiple antibiotic residues in milk, Biosens. Bioelectron. 72 (2015) 320–325, https://doi.org/10.1016/j.bios.2015.05.018.
[13] X. Chen, et al., Portable fluorescent film and gel microspheres for sensitive multi-color detection and efficient adsorption of tetracycline, Separ. Purif. Technol. 352 (2025/01/01/2025) 128258, https://doi.org/10.1016/j.seppur.2024.128258.
[14] Y. Wang, et al., A colorimetric biosensor using Fe_3O_4 nanoparticles for highly sensitive and selective detection of tetracyclines, Sensor. Actuator. B Chem. 236 (2016) 621–626, https://doi.org/10.1016/j.snb.2016.06.029.
[15] L. Jia, et al., A stick-like intelligent multicolor nano-sensor for the detection of tetracycline: the integration of nano-clay and carbon dots, J. Hazard Mater. 413 (2021/07/05/2021) 125296, https://doi.org/10.1016/j.jhazmat.2021.125296.
[16] L. Zhang, et al., Portable luminescent fiber- and glove-based nanosensor for multicolor visual detection of tetracycline in food samples, Microchim. Acta 191 (4) (2024/04/01 2024) 225, https://doi.org/10.1007/s00604-024-06306-3.
[17] F. Yue, et al., A dual-channel sensing platform for the cross-interference-free detection of tetracycline and copper ion, Talanta 279 (2024/11/01/2024) 126617, https://doi.org/10.1016/j.talanta.2024.126617.
[18] Y. Yuan, et al., Intelligent detection of tetracycline by a rare earth multicolor fluorescent probe based on guanosine-5′-monophosphate, Colloids Surf. A Physicochem. Eng. Asp. 688 (2024) 133613, https://doi.org/10.1016/j.colsurfa.2024.133613.
[19] J. Xu, et al., A multi-color fluorescent sensing system integrated with color recognition, liquid crystal display, and voice output module for intelligent detection of two targets, Appl. Surf. Sci. 653 (2024/04/30/2024) 159436, https://doi.org/10.1016/j.apsusc.2024.159436.
[20] J. Xu, B. Zhang, L. Jia, N. Bi, T. Zhao, Metal-enhanced fluorescence detection and degradation of tetracycline by silver nanoparticle-encapsulated halloysite nano-lumen, J. Hazard Mater. 386 (2020) 121630, https://doi.org/10.1016/j.jhazmat.2019.121630.
[21] F. Fernández, F. Sánchez-Baeza, M.-P. Marco, Nanogold probe enhanced surface plasmon resonance immunosensor for improved detection of antibiotic residues, Biosens. Bioelectron. 34 (1) (2012) 151–158, https://doi.org/10.1016/j.bios.2012.01.036.
[22] Z. Liu, J. Hou, Q. He, X. Luo, D. Huo, C. Hou, New application of Mn-doped ZnS quantum dots: phosphorescent sensor for the rapid screening of chloramphenicol and tetracycline residues, Anal. Methods 12 (27) (2020) 3513–3522, https://doi.org/10.1039/D0AY00961J.
[23] S. H. Nguyen, V.-N. Nguyen, and M. T. Tran, "Simple Fluorescent Sensors Based on ZnS-Doped Mn Capped Chitosan Nanomaterials to Detect Ampicillin," in *Optica Imaging Congress 2024 (3D, AOMS, COSI, ISA, pcAOP)*, Toulouse, 2024/07/15 2024: Optica Publishing Group , in Technical Digest Series, p. JD6A.3, doi: 10.1364/3D.2024.JD6A.3. [Online]. Available: https://opg.optica.org/abstract.cfm?URI=3D-2024-JD6A.3.
[24] Y. Jiang, J. Wu, Recent development in chitosan nanocomposites for surface-based biosensor applications, Electrophoresis 40 (16–17) (2019) 2084–2097, https://doi.org/10.1002/elps.201900066.
[25] S.H. Nguyen, V.-N. Nguyen, M.T. Tran, Dual-channel fluorescent sensors based on chitosan-coated Mn-doped ZnS micromaterials to detect ampicillin, Sci. Rep. 14 (1) (2024/05/02 2024) 10066, https://doi.org/10.1038/s41598-024-59772-3.
[26] S.H. Nguyen, V.-N. Nguyen, M.T. Tran, Ampicillin detection using absorbance biosensors utilizing Mn-doped ZnS capped with chitosan micromaterials, Heliyon 10 (10) (2024/05/30/2024) e31617, https://doi.org/10.1016/j.heliyon.2024.e31617.
[27] O.H. Shayesteh, R. Ghavami, Two colorimetric ampicillin sensing schemes based on the interaction of aptamers with gold nanoparticles, Microchim. Acta 186 (2019) 1–10, https://doi.org/10.1007/s00604-019-3524-4.

[28] S.H. Nguyen, P.K.T. Vu, M.T. Tran, Absorbance biosensors-based hybrid MoS_2 nanosheets for *Escherichia coli* detection, Sci. Rep. 13 (1) (2023) 10235, https://doi.org/10.1038/s41598-023-37395-4.
[29] S.H. Nguyen, P.K.T. Vu, M.T. Tran, Glucose sensors based on chitosan capped Zns doped Mn nanomaterials, IEEE Sensors Letters 7 (2) (2023) 1–4, https://doi.org/10.1109/LSENS.2023.3240240.
[30] S.H. Nguyen, P.K.T. Vu, H.M. Nguyen, M.T. Tran, Optical glucose sensors based on chitosan-capped ZnS-doped Mn nanomaterials, Sensors 23 (5) (2023) 2841, https://doi.org/10.3390/s23052841.
[31] A.L. Efros, M. Rosen, The electronic structure of semiconductor Nanocrystals1, Annu. Rev. Mater. Res. 30 (30) (2000) 475–521, https://doi.org/10.1146/annurev.matsci.30.1.475, 2000.
[32] D.D. Drozd, et al., Enhancement of the alloyed CdZnSeS/ZnS quantum dots photoluminescence by thiol ligands capping, Chem. Eng. J. 492 (2024/07/15/2024) 152278, https://doi.org/10.1016/j.cej.2024.152278.
[33] H. Raghuram, S. Pradeep, S. Dash, R. Chowdhury, S. Mazumder, Chitosan-encapsulated ZnS: m (m: Fe^{3+} or Mn^{2+}) quantum dots for fluorescent labelling of sulphate-reducing bacteria, Bull. Mater. Sci. 39 (2016) 405–413, https://doi.org/10.1007/s12034-016-1178-y.
[34] L. Zhang, L. Chen, Fluorescence probe based on hybrid mesoporous silica/quantum dot/molecularly imprinted polymer for detection of tetracycline, ACS applied materials & interfaces 8 (25) (2016) 16248–16256, https://doi.org/10.1021/acsami.6b04381.
[35] S. Yang, et al., A label-free fluorescent biosensor based on specific aptamer-templated silver nanoclusters for the detection of tetracycline, J. Nanobiotechnol. 21 (1) (2023) 22, https://doi.org/10.1186/s12951-023-01785-7.
[36] M. Ramezani, N.M. Danesh, P. Lavaee, K. Abnous, S.M. Taghdisi, A novel colorimetric triple-helix molecular switch aptasensor for ultrasensitive detection of tetracycline, Biosens. Bioelectron. 70 (2015) 181–187, https://doi.org/10.1016/j.bios.2015.03.040.
[37] A. Benvidi, M.D. Tezerjani, S.M. Moshtaghiun, M. Mazloum-Ardakani, An aptasensor for tetracycline using a glassy carbon modified with nanosheets of graphene oxide, Microchim. Acta 183 (2016) 1797–1804, https://doi.org/10.1007/s00604-016-1810-y.